



Benchmark comparison study for mantle thermal convection using the CitcomCU numerical code

Jamison Assunção (IAG, USP)* and Victor Sacek (IAG, USP)

Copyright 2017, SBGf - Sociedade Brasileira de Geofísica

This paper was prepared for presentation during the 15th International Congress of the Brazilian Geophysical Society held in Rio de Janeiro, Brazil, 31 July to 3 August, 2017.

Contents of this paper were reviewed by the Technical Committee of the 15th International Congress of the Brazilian Geophysical Society and do not necessarily represent any position of the SBGf, its officers or members. Electronic reproduction or storage of any part of this paper for commercial purposes without the written consent of the Brazilian Geophysical Society is prohibited.

Abstract

The mathematical approach for mantle studies relies on both analytical and numerical methods, but the absence of known analytical solutions for most of the scenarios makes a wide variety of numerical codes that cannot be easily tested. For these codes to be tested, there is a benchmark, which will provide comparison data from different researchers. This data is presented as a single result with deviation calculated with the similar data provided by the researchers. These benchmarks set standard models. This benchmark comparison study contains numerical simulations calculated using the 3D finite element parallel code CitcomCU for mantle thermal and thermochemical convection reproducing some of the benchmark cases proposed by Blankenbach et al. (1989). The mantle is treated as an inelastic, uncompressible and viscous fluid using the Boussinesq approximation with an infinite Prandtl number. This benchmark comparison allowed to verify the reliability of the numerical code for qualitative studies and observed limitations of the code were presented for a better quantitative result. The numerical solutions indicate that the linear interpolation of the thermal structure between the nodes results in larger deviations mainly in zones with relatively high gradient. The proposed method to this would be to increase the grid resolution in those zones seeking for a balance between grid resolution and consequent simulation run time.

Introduction

There are two main ways to study mantle thermal convection problems with a mathematical approach. The first one is through analytical approach making it to be possible to predict the behavior of the mantle applying fluid mechanics theory. The difficulty of this approach is associated with the absence of known solutions in most cases. Therefore, this approach can only be used for simple studies of the mantle. The second mathematical approach is the numerical approach, where we can use codes based on the fluid mechanics theory to give approximations of the behavior of the mantle in a discretized space and time scenario.

What must be a concern dealing with numerical codes is how to evaluate its applicability to solve certain problems. The accuracy and precision of the numerical method must

be studied to allow data reliability. The so-called benchmarks play this study role allowing researchers to team up and compare their codes through statistics, proposing pre-defined simulations seeking similar results. Once published, these results can be useful for other researchers to validate their codes and, because of that, the scenario simulated by them can be considered for mantle understanding.

This work has the objective to test the 3D finite element parallel code CitcomCU from the Computational Infrastructure for Geodynamics (CIG) team modified from the original Citcom code from Moresi and Gurnis (1996), while comparing its results with the results obtained by Blankenbach et al. (1989) benchmark. While doing this, the found limitations of the CitcomCU will be presented as a way of helping further research in mantle dynamic problems using the CitcomCU code.

Method

CitcomCU is a modification from the original code Citcom from Moresi and Gurnis (1996) written in C programming language and under the GNU General Public License of free usage. It works with a file of initial conditions which contains the geometric and physical information such as the Rayleigh number (Ra), boundary conditions and initial thermal state. All these required parameters are non-dimensional.

These parameters were defined for each one of the Blankenbach et al. (1989) studied cases which will be described ahead. In Blankenbach et al (1989) the models are 2D thermal convections of a non-rotating fluid with infinite Prandtl number using the Boussinesq approximation in rectangular cells. As the CitcomCU is a 3D numerical code, the extra dimension of the simulation was defined in every case as being narrow and invariant, that is, the temperature and velocity gradients in that direction were set to be null in the initial file.

The chosen cases from Blankenbach et al. (1989) were the cases 1a, 2a, 2b, 3 and 3'. The physical parameters are listed in Table 1.

To qualify the CitcomCU code, it is necessary to make comparison studies. The first one is the qualitative study, verifying if the scenarios are similar enough to the one it will be compared to. The second is the quantitative study, making it possible to compare specific values and their deviations from the values from a benchmark.

For the simulated cases, the following values were requested for a quantitative comparison: (i) the non-dimensional Nusselt Number Nu , (ii) the non-dimensional root mean square velocity v_{rms} , (iii) the non-dimensional temperature gradient Q_i in the positions $Q_1(0, y, \Delta z)$, $Q_2(\Delta x, y, \Delta z)$, $Q_3(\Delta z, y, 0)$ and $Q_4(0, y, 0)$, (iv) the dynamic

topography at the top of the cell $\xi_1(x = 0)$ and $\xi_2(x = \Delta x)$, (v) the dynamic topography at the bottom of the cell $\xi_3(x = 0)$ and $\xi_4(x = \Delta x)$ and (vi) the x value (function of b) of the intersection between the topography curve and the zero curve, where the zero was defined as the mean dynamic topography of that simulation.

Table 1 – Properties, symbols and values.

Property	Symbol	Value (SI)
Density	ρ	4000
Gravity	g	10
Thermal expansion coefficient	α	2.5×10^{-5}
Height of the cell	b	10^6
Kinematic viscosity at surface	ν_0	2.5×10^{19}
Thermal diffusivity	κ	1.0×10^{-6}
Temperature contrast	ΔT	1000.0
Surface temperature	T_0	0.0
Volumetric rate of internal heating	q	5.0×10^{-9}
Thermal capacity	c_p	1.25×10^3
Horizontal length of the cell	Δx	1.0b (Case 1a) 1.0b (Case 2a) 2.5b (Case 2b) 1.5b (Case 3 and 3')
Vertical length of the cell	Δz	1.0b

With the geometry of the cells described in Table 1, the benchmark cases are:

Case 1a. Convection is steady and the viscosity is constant in a square box, where the temperature is zero on top of the cell and ΔT on the bottom with no internal heat sources. The sidewalls are symmetrically reflective and therefore $\partial T / \partial x = 0$. All boundaries are absent of stresses and the $Ra = 10000$. To understand how the grid size affects the result, three sizes were used: $(65 \times 2 \times 65)$, $(33 \times 2 \times 33)$ and $(17 \times 2 \times 17)$. These sizes represent the number of nodes each grid has in each coordinate component ($x \times y \times z$).

Case 2. This case has all boundary conditions as Case 1a except that now viscosity is temperature- and depth-dependent as illustrated in equation 1.

$$\nu = \nu_0 \exp \left[\frac{\beta T}{\Delta T} + \frac{\gamma(1-z)}{b} \right] \quad (1)$$

where for Case 2a, $\beta = \ln(1000)$ and $\gamma = 0$ with $Ra = 10000$. For case 2b, $\beta = \ln(16384)$ and $\gamma = \ln(64)$ with $Ra = 10000$. The different grid sizes used were: $(73 \times 2 \times 73)$, $(37 \times 2 \times 37)$ and $(19 \times 2 \times 19)$.

Case 3. This case consists of a time-dependent convection with constant viscosity and internal heat source. Tangential velocity at the top and bottom of the cell is null. The top is an isothermal with $T = 0$ and at the bottom the gradient $\partial T / \partial z = 0$. The reflective symmetry is still adopted and the Rayleigh number is defined as

$$Ra = \frac{\alpha g q b^5}{\kappa^2 \rho c_p \nu} = 216000 \quad (2)$$

For the Case 3', Ra was considered to be 218000. The size of the grid in both these last two cases was $(97 \times 3 \times 65)$.

It is important for a simulation to define the initial temperature configuration for the simulation to run. This will increase the convergence of the simulation and, more importantly, will give an initial scenario to observe its evolution. For Case 1a the initial temperature configuration was not needed because of its simplicity. For Case 2a and 2b the following was done: from a vertical linear temperature variation, a temperature $T^*(x, z)$ was added as shown in equation 3 as proposed in Turcotte and Scubert (2002).

$$T^*(x, z) = T_0^* \cos \left(\frac{\pi z}{b} \right) \cos \left(\frac{2\pi x}{\lambda} \right) \quad (3)$$

where x and z are the coordinates (note that it does not depend on the y coordinate), T_0^* is the non-dimensional amplitude of the added temperature and λ is the non-dimensional wavelength of the added temperature function. In both Cases 2a and 2b λ was defined to be $2\Delta x$ and $T_0^* = 0.1$ to generate a single convection cell.

For the Case 3 and 3', the initial temperature configuration was set to be the result of the Case 2a. Therefore, the initial temperature scenarios is already of a single developed convection cell.

Results

Case 1a. The results of the simulation are presented in Table 3 with the reference Blankenbach results in Table 2. Relatively higher Q_1 , Q_2 and Nu are observed.

Table 2 – Results for Case 1a with deviations adapted from Blankenbach et al. (1989).

Parameter	Value
Nu	4.884409 ± 0.000010
v_{rms}	42.864947 ± 0.000020
Q_1	8.059384 ± 0.000003
Q_2	0.588810 ± 0.000003
ξ_1	2254.022 ± 0.050
ξ_2	-2903.230 ± 0.050
$x(\xi = 0)$	0.539372 ± 0.000030

Table 3 - Calculated values for each grid size G_{17} , G_{33} and G_{65} , with $(17 \times 2 \times 17)$, $(33 \times 2 \times 33)$ and $(65 \times 2 \times 65)$ nodes, respectively, and the percentage difference of the values from Blankenbach et al. (1989) for Case 1a.

Grid	Parameter	Value	Difference (%)
G_{17}	Nu	4.485957	8.16
	v_{rms}	42.995191	-0.30
	Q_1	7.273424	9.75
	Q_2	0.54722	7.06
	ξ_1	2327.033	-3.24
	ξ_2	-2913.002	-0.34
	$x(\xi = 0)$	0.529412	1.85
	G_{33}	Nu	4.784567
v_{rms}		42.957696	-0.22
Q_1		7.839936	2.72
Q_2		0.57568	2.23
ξ_1		2279.865	-1.15
ξ_2		-2911.505	-0.29
$x(\xi = 0)$		0.515152	4.49
G_{65}		Nu	4.857444
	v_{rms}	42.871608	-0.02
	Q_1	8.000000	0.74
	Q_2	0.585494	0.56
	ξ_1	2264.419	-0.46
	ξ_2	-2903.338	0.00
	$x(\xi = 0)$	0.538462	0.17

Case 2a. The results for Case 2a are shown in Table 5 with the benchmark reference values presented in Table 4.

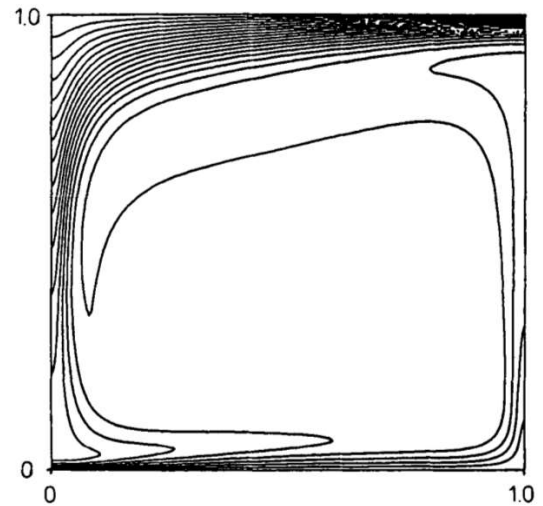
Table 4 - Results for Case 1a with deviations adapted from Blankenbach et al. (1989).

Parameter	Value
Nu	10.0660 ± 0.0002
v_{rms}	480.4334 ± 0.1000
Q_1	17.53136 ± 0.00400
Q_2	1.00851 ± 0.00020
Q_3	26.8085 ± 0.0100
Q_4	0.497380 ± 0.000100
ξ_1	1010.92 ± 0.20
ξ_2	-4098.09 ± 0.80
$x_1(\xi = 0)$	0.67700 ± 0.00005
ξ_3	386.38 ± 0.10
ξ_4	-788.10 ± 0.50
$x_2(\xi = 0)$	0.6308 ± 0.00020

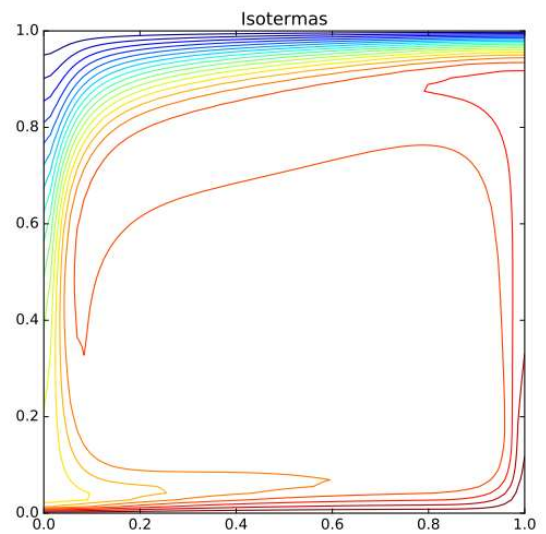
Table 5 - Calculated values for each grid size G_{19} , G_{37} and G_{73} , with $(19 \times 2 \times 19)$, $(37 \times 2 \times 37)$ and $(73 \times 2 \times 73)$ nodes, respectively, and the percentage difference of the values from Blankenbach et al. (1989) for Case 2a.

Grid	Parameter	Value	Difference (%)
G_{19}	Nu	8.8778	11.80
	v_{rms}	563.5285	-17.30
	Q_1	14.67090	16.32
	Q_2	1.0	-0.47
	Q_3	5.0216	81.27
	Q_4	0.276714	44.37
	ξ_1	1174.06	-16.14
	ξ_2	-3450.71	15.80
	$x_1(\xi = 0)$	0.63158	6.71
	ξ_3	382.32	1.05
G_{37}	ξ_4	-449.80	42.93
	$x_2(\xi = 0)$	0.52632	16.57
	Nu	9.6877	3.76
	v_{rms}	496.8795	-3.42
	Q_1	16.82377	4.04
	Q_2	0.96513	4.30
	Q_3	12.7797	52.33
	Q_4	0.410976	17.37
	ξ_1	1104.14	-9.22
	ξ_2	-3886.97	5.15
G_{73}	$x_1(\xi = 0)$	0.67568	0.19
	ξ_3	413.77	-7.09
	ξ_4	-696.56	11.62
	$x_2(\xi = 0)$	0.62162	1.46
	Nu	9.9647	1.01
	v_{rms}	484.6638	-0.88
	Q_1	17.326584	1.17
	Q_2	0.99516	1.32
	Q_3	22.0749	17.66
	Q_4	0.508032	-2.14
G_{73}	ξ_1	1046.02	-3.47
	ξ_2	-4041.7	1.38
	$x_1(\xi = 0)$	0.67123	0.85
	ξ_3	401.08	-3.80
	ξ_4	-799.00	-1.38
	$x_2(\xi = 0)$	0.63014	0.11

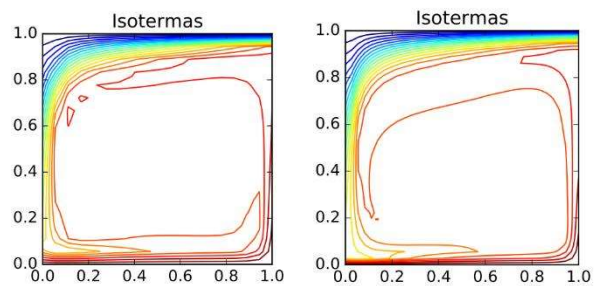
Figure (1) shows all the simulated cases at their stationary solution. The scenarios can be compared to the Blankenbach et al. (1989) result shown in Figure (1a).



(a) Isotherms with $\Delta T/20$ discretization for Case 2a adapted from Blankenbach et al. (1989).



(b) Isotherms with $\Delta T/20$ spacing for Case 2a with $(73 \times 2 \times 73)$ nodes.



(c) Isotherms with $\Delta T/20$ spacing for Case 2a with grid of $(17 \times 2 \times 17)$ nodes (left image) and $(33 \times 2 \times 33)$ nodes (right image).

Figure 1 – Isotherms for the Case 2a from Blankenbach et al (1989) and the simulated cases with lines every interval of $\Delta T/20$.

Case 2b. The reference benchmark values can be seen in Table 5 and the results of the simulations for the Case 2b are shown in Table 6 for each grid size.

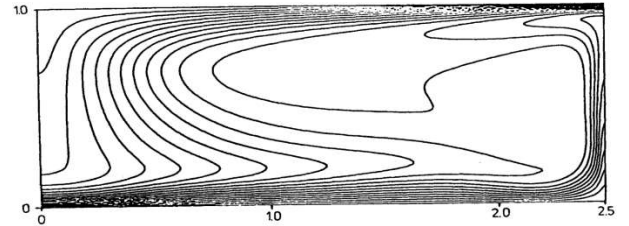
Table 6 - Blankenbach et al. (1989) results for Case 2b with deviations.

Parameter	Value
Nu	6.9299 ± 0.0005
v_{rms}	171.755 ± 0.020
Q_1	18.4842 ± 0.0100
Q_2	0.17742 ± 0.00003
Q_3	14.1682 ± 0.0050
Q_4	0.61770 ± 0.00005
ξ_1	1538.8 ± 3.0
ξ_2	-4341.5 ± 1.5
$x_1(\xi = 0)$	1.6358 ± 0.0030
ξ_3	2311.8 ± 1.0
ξ_4	-6639.70 ± 3.0
$x_2(\xi = 0)$	1.7311 ± 0.0005

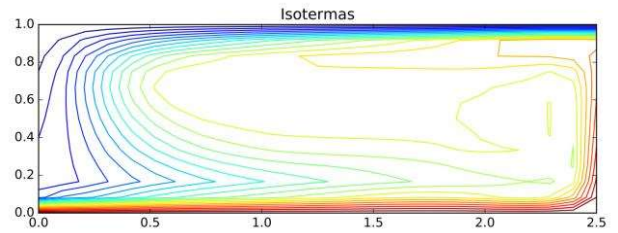
Table 7 - Calculated values for each grid size $G_{25 \times 13}$, $G_{49 \times 25}$ and $G_{97 \times 49}$, with $(25 \times 2 \times 13)$, $(49 \times 2 \times 25)$ and $(97 \times 2 \times 49)$ nodes, respectively, and the percentage difference of the values from Blankenbach et al. (1989) for Case 2b.

Grid	Parameter	Value	Difference (%)
$G_{25 \times 13}$	Nu	5.5929	19.29
	v_{rms}	199.761	-16.31
	Q_1	8.79690	52.41
	Q_2	0.22468	-26.64
	Q_3	9.8837	30.24
	Q_4	0.59396	3.84
	ξ_1	1412.9	8.18
	ξ_2	-4651.7	-7.14
	$x_1(\xi = 0)$	1.7000	-3.92
	ξ_3	2392.9	-3.51
	ξ_4	-7406.50	-11.55
	$x_2(\xi = 0)$	1.8000	-3.98
	$G_{49 \times 25}$	Nu	6.2775
v_{rms}		182.257	-6.11
Q_1		15.3724	16.83
Q_2		0.17590	0.86
Q_3		11.9710	15.51
Q_4		0.60026	2.82
ξ_1		1623.8	-5.52
ξ_2		-4431.0	-2.06
$x_1(\xi = 0)$		1.6327	0.19
ξ_3		2421.0	-4.72
ξ_4		-6892.9	-3.81
$x_2(\xi = 0)$		1.7347	-0.21
$G_{97 \times 49}$		Nu	6.7545
	v_{rms}	174.448	-1.57
	Q_1	17.8582	3.39
	Q_2	0.17681	0.34
	Q_3	13.3011	6.12
	Q_4	0.57538	6.85
	ξ_1	1597.2	-3.80
	ξ_2	-4362.9	-0.49
	$x_1(\xi = 0)$	1.6237	0.74
	ξ_3	2352.7	-1.77
	ξ_4	-6680.10	-0.61
	$x_2(\xi = 0)$	1.7268	0.25

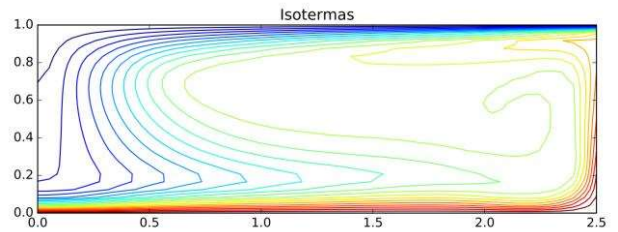
Figure (2a) shows the Blankenbach et al. (1989) stationary solution and Figures (2b), (2c) and (2d) show the stationary solutions found with CitcomCU.



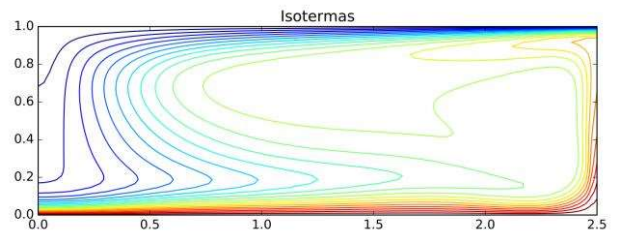
(a) Isotherms with $\Delta T/20$ spacing from Blankenbach et al. (1989) for Case 2b.



(b) Isotherms with $\Delta T/20$ spacing for Case 2b and grid with $(25 \times 2 \times 13)$ nodes.



(c) Isotherms with $\Delta T/20$ spacing for Case 2b and grid with $(49 \times 2 \times 25)$ nodes.



(d) Isotherms with $\Delta T/20$ spacing for Case 2b and grid with $(97 \times 2 \times 49)$ nodes.

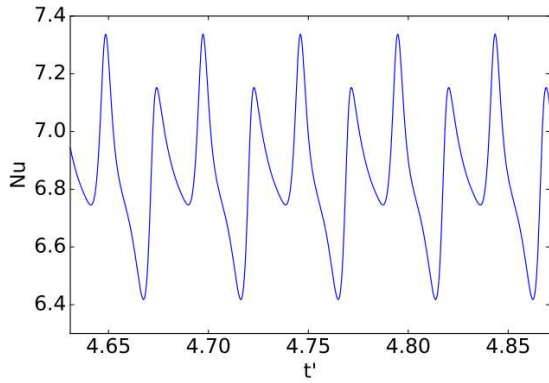
Figure 2 – Isotherms for the Case 2b from Blankenbach et al (1989) and the simulated cases with lines every interval of $\Delta T/20$.

Case 3. The results of the Case 3 simulations are shown in Table 8 compared with the Blankenbach et al. (1989) value.

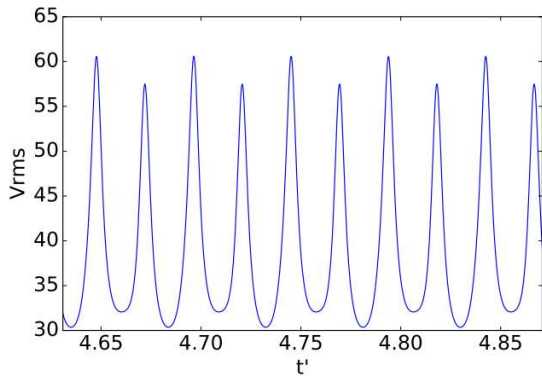
Table 8 – Simulation results for Case 3 from Blankenbach et al. (1989) with percentage difference for the grid with (97×3×65) nodes.

Parameter	CitcomCU	Blankenbach et al. (1989)	Difference (%)
Period	0.05003	0.04803 ± 0.00003	-4.16
$Nu_{max,1}$	7.292	7.379 ± 0.005	1.18
$Nu_{min,1}$	6.353	6.468 ± 0.005	1.78
$Nu_{max,2}$	7.192	7.196 ± 0.005	0.06
$Nu_{min,2}$	6.735	6.769 ± 0.005	0.50
$v_{rms,max,1}$	61.768	60.367 ± 0.015	-2.32
$v_{rms,min,1}$	32.022	31.981 ± 0.020	-0.13
$v_{rms,max,2}$	56.11	57.43 ± 0.05	2.30
$v_{rms,min,2}$	30.48	30.32 ± 0.05	-0.53

Figure (3a) and (3b) shows the periodic behavior through time of a P2 cycle where there are two maximums and minimums in the Nusselt Number and in the v_{rms} profiles. Figure (4) show the relationship between these two values.



(a) Nu profile as function of the time t' .



(b) v_{rms} profile as function of the time t' .

Figure 3 – Nu and v_{rms} graphs for Case 3.

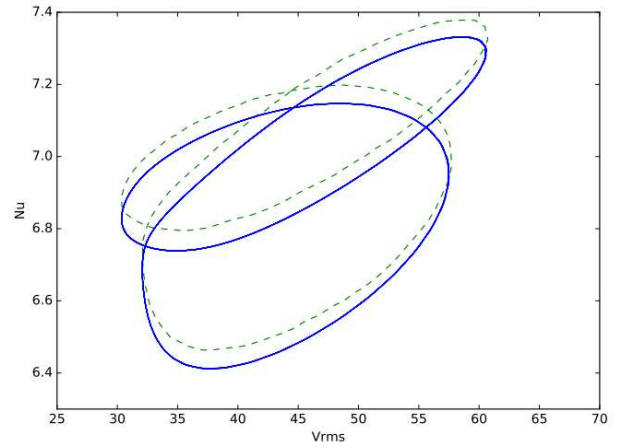


Figure 4 – $Nu \times v_{rms}$ graph comparison between the values obtained with the CitcomCU (blue line) and the values from Blankenbach et al. (1989) (green dashed line) for Case 3.

Figure (4) presents a shift from the Blankenbach et al. (1989) case, suggesting a common deviation for the Nu .

Case 3'. The results of the Case 3' are shown in Table 9 compared with the Blankenbach et al. (1989) values. This case is a condition case from Blankenbach et al. (1989). That means it should be simulated only if the Case 3 result was satisfactory.

Table 9 – Simulation results for Case 3' from Blankenbach et al. (1989) with percentage difference for the grid with (97×3×65) nodes.

Parameter	CitcomCU	Blankenbach et al. (1989)	Difference (%)
Period	0.09696	0.09568	-1.33779
$Nu_{max,1}$	7.3462	7.3825	0.491703
$Nu_{min,1}$	6.4584	6.5053	0.720951
$Nu_{max,2}$	7.3395	7.3837	0.598616
$Nu_{min,2}$	6.3809	6.4229	0.65391
$Nu_{max,3}$	7.2145	7.2606	0.634934
$Nu_{min,3}$	6.7901	6.8401	0.730983
$Nu_{max,4}$	7.0910	7.1232	0.452044
$Nu_{min,4}$	6.7192	6.7588	0.585903
$v_{rms,max,1}$	61.3607	61.854	0.797523
$v_{rms,min,1}$	32.0791	32.370	0.898672
$v_{rms,max,2}$	60.2075	60.619	0.67883
$v_{rms,min,2}$	32.3774	32.46	0.254467
$v_{rms,max,3}$	59.0851	59.567	0.809005
$v_{rms,min,3}$	30.4233	30.455	0.104088
$v_{rms,max,4}$	56.1676	56.058	-0.19551
$v_{rms,min,4}$	30.5602	30.603	0.139856

Figure (5) shows the $Nu \times v_{rms}$ graph for the Case 3'.

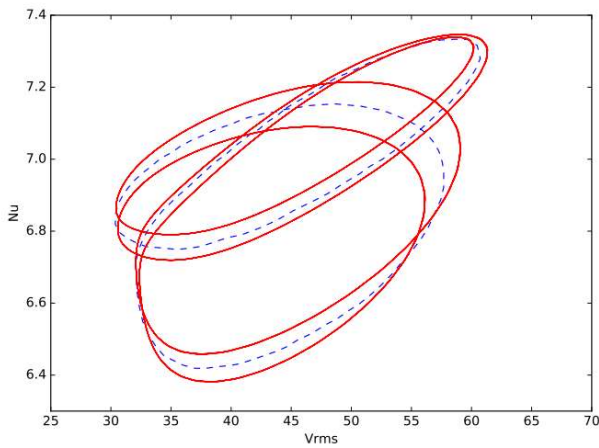


Figure 5 – $Nu \times v_{rms}$ graph for the Case 3' (red line) compared with the values obtained in Case 3 with CitcomCU (blue dashed line).

Conclusions

The 3D finite element parallel code CitcomCU presented good results for the Blankenbach et al. (1989) benchmark cases. It is important to point out that the calculated values for the temperature gradient were more unsatisfactory, therefore, to produce better results, a more refined grid is necessary when such data is required. It is recommended to make a first simulation with a small number of grid elements and then, once the high gradient zones are identified, make another simulation with smaller elements in those zones.

CitcomCU uses a linear interpolation for the discrete data, which must be associated with this limitation of the gradient calculation. The observed shift in the third case is also related to this.

In a general way, the code presented better results for higher grid resolution. The possible deviations from this conclusion must be associated with coincidence due to the zones with complex behavior with low resolution grid.

The Case 3' is also an argument in favor of the utilized numerical code, once it should be done only if the Case 3 results were satisfactory (which they were) and the Case 3' present very good results as well.

The general behaviors of the simulations were very close to those observed in the benchmark, which makes CitcomCU a good code for a qualitative study. The concern one must have is to produce reliable data of complex and high gradient scenarios balancing the grid size and the time for simulation to run. Once this balance is done, the CitcomCU is an excellent code for quantitative study as well.

References

BLANKENBACH, B.; BUSSE, F.; CHRISTENSEN, U.; CSEREPES, L.; GUNKEL, D.; HANSEN, U.; HARDER, H.; JARVIS, G.; KOCH, M.; MARQUART, G.; MOORE, D.; OLSON, P.; SCHMELING, H. & SCHNAUBELT, T. 1989. A benchmark comparison for mantle convection codes. *Geophysical Journal International*, v.98(1), 23-38 p.

MORESI, L. & GURNIS, M. 1996. Constraints on the lateral strength of slabs from three-dimensional dynamic flow models. *Earth and Planetary Science Letters*. V 138(1), 15-28 p.

TURCOTTE, D. L. & SCHUBERT, G. 2002. *Geodynamics*, pp 456. Cambridge University Press.